Bound Photonic Pairs in 2D Waveguide Quantum Electrodynamics

Y. Marques,[1] I. A. Shelykh,[1,2] and I. V. Iorsh[1,*]
[1]*ITMO University, St. Petersburg 197101, Russia*
[2]*Science Institute, University of Iceland, Dunhagi-3, IS-107 Reykjavik, Iceland*

(Received 8 August 2021; accepted 9 December 2021; published 29 December 2021)

We theoretically predict the formation of two-photon bound states in a two-dimensional waveguide network hosting a lattice of two-level atoms. The properties of these bound pairs and the exclusive domains of the parameter space where they emerge due to the interplay between the on-site photon blockade and peculiar shape of polariton dispersion resulting from the long-range radiative couplings between the qubits are investigated in detail. In addition, we analyze the effect of the finite-size system on localization characteristics of these excitations.

DOI: 10.1103/PhysRevLett.127.273602

Introduction.—The recent development of nanotechnology resulted in the appearance of unprecedented platforms for many-body quantum electrodynamics consisting of quantum emitters coupled to propagating photons in waveguides [1–4]. Particular realizations of such waveguide quantum electrodynamics (WQED) systems include structures based on artificial arrays of cold atoms [5,6], superconducting qubits [7,8], quantum dots [9], and solid-state vacancy defects [10]. The exquisiteness of WQED systems is that they demonstrate an interplay of strong light-matter interaction, chirality, and long-range radiative couplings between quantum emitters arising from the exchange of the propagating photons. The combination of these features gives rise to a plethora of fascinating physical phenomena, including collective super-radiance and subradiance [11–18], the emergence of unconventional topological phases [19,20], and quantum chaos [21], and promotes insightful developments for emergent quantum technologies.

Long-range coherent photonic propagation in a waveguide couples all emitters together and leads to the formation of collective polaritonic excitations [4]. Since a given emitter can be excited only by a single photon, such structure represents an example of a strongly correlated system [22]. One of its most compelling properties is the possibility of the formation of unconventional multiphoton bound states, attracting the growing interest of theoretical researchers [16,23–26]. To date, most of the efforts have been dedicated to the consideration of one-dimensional (1D) setups since they were the only ones accessible experimentally. However, very recently a two-dimensional (2D) network of waveguide-coupled array of transmon qubits was realized [27], which makes relevant the task of the proper theoretical description of a strongly correlated WQED system in higher dimensions. It should be noted that, while the dynamics of single qubits [28] and qubit arrays [29] in two-dimensional photonic reservoirs has been considered previously, the existence of the multiphoton bound states in 2D setups remains an open question. Moreover, this is totally unclear what are their localization characteristics of these bound states in case of their existence.

In this Letter, we explore the formation of the bound two-polariton states in the 2D WQED setup shown in Fig. 1. We show that the bound states indeed exist inside the band gap for the scattering states and establish their spatial profiles. We also demonstrate the characteristics of these polariton pairs in finite-size systems, which can be detected in scattering experiments.

Two-particle Hamiltonian.—We consider the system schematically shown in Fig. 1. It consists of an $N \times N$ square lattice of qubits located at the nodes of a network composed of a set of horizontal and vertical identical one-dimensional waveguides in the xy plane. Each qubit, described as a dipole with resonant frequency ω_0 between

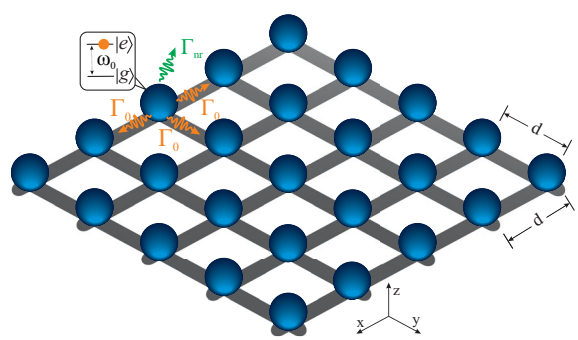

FIG. 1. Sketch of the considered setup consisting of a square lattice of regularly spaced qubits placed over a two-dimensional network of waveguides. The qubits, two-level atoms with resonant frequency ω_0 between ground $|g\rangle$ and excited $|e\rangle$ states, couple with identical waveguides and display the equivalent emission decay rate Γ_0 in both the x and y directions. The nonradiative emission decay rate Γ_{nr} addresses the losses from the scattered photons to the vacuum.

 © 2021 American Physical Society

ground $|g\rangle$ and excited $|e\rangle$ states, couples with a pair of waveguides that support propagating light modes with linear dispersion with velocity v. Waveguide photonic modes can be integrated out in the Markovian regime [11,13,25]. We assume equal probability of a qubit decay into each of the two waveguides, and the corresponding 2D Hamiltonian is given by

$$\mathcal{H}_{\rm eff}^{\rm 2D} = \mathcal{H}_{\rm eff}^{\rm 1D} \otimes I + I \otimes \mathcal{H}_{\rm eff}^{\rm 1D}, \tag{1}$$

where $\mathcal{H}_{\rm eff}^{\rm 1D}$ is the effective 1D Hamiltonian that describes each single waveguide array. For each waveguide, the Hamiltonian describes an open quantum system where the coherent exchange of photons enables an infinite-range qubit-qubit interaction:

$$\mathcal{H}_{\rm eff}^{\rm 1D} = \sum_{m,n=1}^{N} H_{mn} b_m^\dagger b_n + \frac{\chi}{2} \sum_{m=1}^{N} b_m^\dagger b_m^\dagger b_m b_m \tag{2}$$

with $H_{mn} = (\omega_0 - i\Gamma_{\rm nr})\delta_{mn} - i\Gamma_0 e^{i\varphi|m-n|}$, where Γ_0 and $\Gamma_{\rm nr}$ respectively stand for the radiative and nonradiative decay rate of a single qubit, $\varphi = q_0 d$ represents the phase acquired by excitations with wave vector $q_0 = \omega_0/v$ when traveling between two qubits spaced by d, the annihilation operators b_m account for the bosonized excitations of the qubits, and χ stems from the effective on-site photon-photon repulsion.

The Eq. (2) Hamiltonian effectively describes the coherent and dissipative collective interaction of the guided modes through $i\Gamma_0 e^{i\varphi|m-n|}$ and also the inherent losses stemming from photon emission to the free space, which is modulated by the nonradiative decay rate $\Gamma_{\rm nr}$. In particular, the waveguide supports guided modes that hardly decay into free space ($\Gamma_{\rm nr}/\Gamma_0 \ll 1$) for small array periods $d < \lambda_0/2$ ($\varphi < \pi$), where $\lambda_0 = 2\pi c/\omega_0$ is the atomic wavelength. At the current level of technology, this high level of the qubit-waveguide coupling is achieved in the systems based on superconducting qubits [8,30]. At the same time, the considered geometry would require a multilayer circuit since the perpendicular waveguides ought to be isolated from each other and be coupled only via the common qubits to suppress the cross talks. Fabrication of the three-level superconducting circuit is a challenging task at the moment, even though the first demonstrations of the multilayer superconducting quantum circuits have recently appeared [31].

As single two-level atoms are prevented from being excited by two identical photons at the same time due to the Pauli exclusion principle, the system lies on the so-called hard-core limit ($\chi \to \infty$) [11,21,25], where the occupation of each qubit, restricted to either 0 or 1, leads to a picture where the light-matter excitations (polaritons) effectively exhibit fermionic behavior [32].

To analyze the nature of two-particle excitations of the 2D lattice, we need to solve the corresponding linear eigenvalue problem written as (see the Supplemental Material [33] for the details):

$$\begin{aligned} 2\varepsilon\psi_{ij,mn} = {} & H_{il}\psi_{lj,mn} + H_{jl}\psi_{il,mn} + H_{ml}\psi_{ij,ln} \\ & + H_{nl}\psi_{ij,ml} - 2\delta_{jn}H_{il}\psi_{lj,in} - 2\delta_{im}H_{jl}\psi_{il,mj}, \end{aligned} \tag{3}$$

where $\psi_{ij,mn}$ denotes the probability amplitude associated with the polariton pair, in which i, j (m, n) indicates the position of first (second) polariton. The indices i, m correspond to the x coordinates' positions, j, n to the y coordinates'.

For an infinite periodic lattice, the polariton pair is characterized by the center of mass wave vector $\boldsymbol{K} = K_x\hat{e}_i + K_y\hat{e}_j$ so that two-particle amplitudes can be written as

$$\psi_{ij,mn} = e^{iK_x(i+m)/2} e^{iK_y(j+n)/2} \Phi_{i-m,j-n}, \tag{4}$$

with the wave function of the relative motion $\Phi_{0,0} = 0$ and $\Phi_{i-m,j-n} = \Phi_{m-i,j-n}$. Substituting Eq. (4) into Eq. (3) and introducing the relative distances $d_x = i - m$ and $d_y = j - n$, we find the system of equations characterizing the relative motion of a polariton pair, which is given by

$$\varepsilon_{\boldsymbol{K}} \Phi_{d_x,d_y} = \sum_{l=-\infty}^{\infty} (H_{l,d_x}\Phi_{l,d_y} + H_{l,dy}\Phi_{d_x,l}), \tag{5}$$

where $H_{l,d\lambda} = -i\Gamma_0 \cos\{K_\lambda[(d_\lambda - l)/2]\} e^{i\varphi|d_\lambda - l|}$ for $\lambda = x$, y. Solutions of Eq. (5) describe both the scattering states corresponding to the continuous part of the spectrum and, under specific conditions, the formation of bound pairs.

In order to obtain the scattering state dispersion relation, we move from the center of mass position basis to the relative motion wave vector $(-\pi < q_x, q_y \leq \pi)$ basis by performing a 2D cosine Fourier transform in Eq. (5). As a result, the system dispersion relation equation is given by

$$\begin{aligned} 2\varepsilon_{q_x,q_y} = {} & \Gamma_0 \left(\frac{\sin\varphi}{\cos k_{1,x} - \cos\varphi} + \frac{\sin\varphi}{\cos k_{2,x} - \cos\varphi} \right) \\ & + \Gamma_0 \left(\frac{\sin\varphi}{\cos k_{1,y} - \cos\varphi} + \frac{\sin\varphi}{\cos k_{2,y} - \cos\varphi} \right). \end{aligned} \tag{6}$$

The total energy of a pair $2\varepsilon_{q_x,q_y}$ is represented as a sum of the energies of noninteracting polaritons with wave vectors $k_{1(2),x(y)} = (q_{x(y)} \pm K_{x(y)})/2$. Its shape is determined by the phase φ and the center of mass wave vector $\mathbf{K}$, and it is shown in Fig. 2(a) for $\varphi = 3\pi/4$, $K_x = \pi$, and $K_y = 0$.

The impossibility of double occupation in a single qubit due to the on-site repulsion ($\chi \to \infty$) seems to suppress any possibility of observing bound state pairs. Nonetheless, the lattice has an infinite-range radiative coupling so that the polariton-polariton correlation, stemming from the on-site repulsion, is preserved all along the lattice. This is essential to the formation of bound states with repulsive interactions perceived by the negative effective mass regions in the

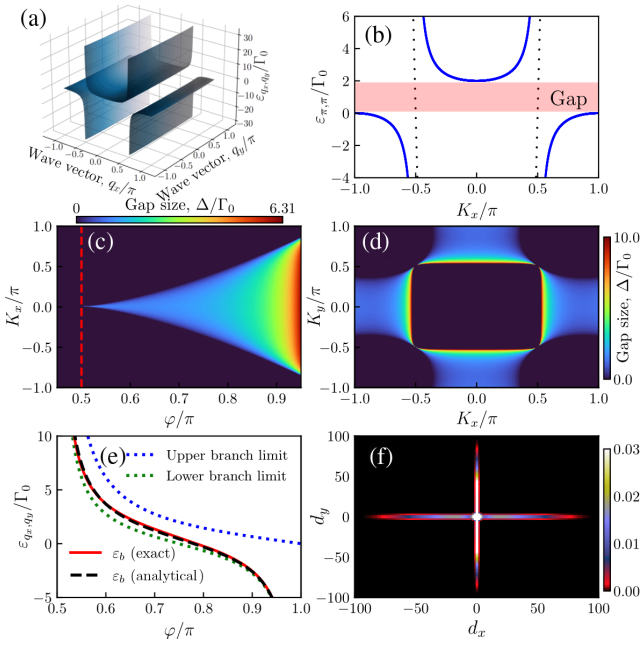

FIG. 2. (a) Polariton dispersion of the two-dimensional lattice for center of mass wave vectors $K_x = \pi$ and $K_y = 0$. (b) 1D slice of the dispersion relation at $K_y = \pi$ considering isotropic polariton wave vectors $q_x = q_y = \pi$. The black dotted lines show the dispersion of light in pristine waveguides. (c),(d) The size of the energy gap in the polariton dispersion for $K_x = \pi$ and $\varphi = 3\pi/4$, respectively. The vertical dashed line in panel (c) highlights the gap opening at $\varphi = \pi/2$. (e) Exact (solid red line) and analytical (black dashed line) bound state energy, where the blue and green dashed curves illustrate the lowest and highest energy values of the upper and lower polariton branches, respectively. (f) Polariton spatial distribution $|\Phi_{d_x,d_y}|^2$ (rescaled by 0.2). The polariton phase is set at $\varphi = 3\pi/4$ in panels (a), (c), (e), and (f).

dispersion relation shown in Figs. 2(a) and 2(b). The different sign effective masses of polaritons at the center and the edge of the Brillouin zone allows for the formation of the in-gap bound two-polariton states with energies lying in the band gap even for the case of repulsive interactions. The creation of these finite-energy bound states by strong repulsive interaction has already been observed in Bose-Hubbard models in optical lattices [34].

As bound states arise as discrete in-gap states, the energy gap in the dispersion relation is the main characteristic that allows the formation of bound states. However, the existence of a gap is not guaranteed for any arbitrary values of φ and $\mathbf{K}$. Figures 2(c) and 2(d) show the domains where two-polariton pairs can be observed by revealing the gap size Δ in the dispersion relation. In Fig. 2(c), obtained for $K_x = \pi$, one can notice that bound states cannot be observed in the range of $\varphi \in [0; \pi/2]$ but arise for the parameter combination lying inside the cone-shaped domain. Figure 2(d) maps Δ for values of the center of mass wave vector $\mathbf{K}$ and fixed $\varphi = 3\pi/4$. The dispersion relation profiles where the energy gap is absent are shown in the Supplemental Material [33]. Given the complexity of Eq. (5), we fix the wave vectors $K_x = \pi$ and $K_y = 0$ henceforth to achieve analytical expressions for the bound state energy and its corresponding wave functions.

Two-polariton bound states.—To obtain the bound state energy ε_b, we assume that the condition for $\Phi_{0,0} = 0$ is due to a scattering potential $\hat{v} = \varepsilon_0 |\Phi_{0,0}\rangle\langle\Phi_{0,0}|$ with $\varepsilon_0 \to +\infty$ applied to the unperturbed Hamiltonian characterizing nearly free polariton propagation with dispersion ε_{q_x,q_y}. Within the Green's function formalism [35], the bound states correspond to the poles of the transfer matrix $\mathcal{T} = \hat{v}(\hat{I} - \hat{G}_0(d_x, d_y)\hat{v})^{-1}$. Hence, at the system origin, where the infinite scattering potential is present, the condition for bound states is given by $\hat{G}_0(0,0) = 0$, i.e.,

$$G_0(0,0) = \int_{-\pi}^{\pi}\int_{-\pi}^{\pi} \frac{dq_x dq_y}{\varepsilon_b - \varepsilon_{q_x,q_y}} = 0. \tag{7}$$

The integral in Eq. (7) can be taken analytically but results in a cumbersome expression involving elliptic integrals of the second and third kind. We therefore resort to the numerical solution. However, an approximate solution can be obtained within certain approximations.

Namely, we first note that the bound state energy should lie in the band gap region, i.e., $\cot\varphi < \varepsilon_b < -\tan\varphi$ for $\varphi \in [\pi/2; \pi]$. Then, we can notice from Fig. 2(a) that dispersion along q_y is weak. We thus can use the fact that $\varepsilon_{q_x,q_y} = \varepsilon(q_x) + \varepsilon'(q_y)$ and substitute average value of $\varepsilon'(q_y)$, $\langle\varepsilon'(q_y)\rangle = (2\pi)^{-1}\int dq_y \varepsilon'(q_y)$ in Eq. (7). This would allow us to obtain an approximate expression for the bound energy for $K_x = \pi$, $K_y = 0$,

$$\varepsilon_b \approx 2\Gamma_0 \cot(2\varphi) + \Gamma_0 \operatorname{arctanh}[\cot(\varphi/2)] \tag{8}$$

as is shown by the solid line in Fig. 2(e). As can be seen, this approximation is very close to one given by numerical solution.

The bound polariton pair wave functions are obtained as

$$\Phi_{d_x,d_y} = \Gamma_0 \int_{-\pi}^{\pi}\int_{-\pi}^{\pi} dq_x dq_y \frac{\cos(q_x d_x + q_y d_y)}{\varepsilon_b - \varepsilon_{q_x,q_y}}, \tag{9}$$

with discrete values of relative distances $d_x, d_y = \{0, 1, 2, \ldots\}$, except for $\Phi_{0,0} = 0$. The solution details can be found in the Supplemental Material [33]. The shape of the entire ensemble of solutions is presented in Fig. 2(f) for arbitrary values of d_x and d_y. We can see that the profile has crosslike structure with greater localization along x axis ($K_x = \pi$) than along y axis ($K_y = 0$). It should be noted that the interaction entangles x and y motion of the qubit pair. This can be demonstrated if we introduce the squared displacements along the two axes $\Delta_{x,y} = d_{x,y}^2 - \langle\Phi|d_{x,y}|\Phi\rangle^2$. The correlation between the two axes

then can be computed as $C_{xy} = \langle \Delta_x \Delta_y \rangle / [\langle \Delta_x \rangle \langle \Delta_y \rangle] - 1$. We have computed the correlation numerically yielding the value $C_{xy} \approx -0.15$, which confirms the emergence of the interaction induced correlation between the x and y axes.

Generally, the eigenstates of WQED structures are classified by their collective decay ratio $\Gamma = -\mathrm{Im}\varepsilon$ in comparison with the single qubit decay rate Γ_0, so that $\Gamma \sim N\Gamma_0$ correspond to superradiant states, $\Gamma \sim \Gamma_0$ correspond to bright states, and $\Gamma \ll \Gamma_0$ correspond to subradiant states. Recently, new classes of eigenstates that emerge exclusively in multiparticle excitation regimes, such as twilight [11], chaotic [21], and bound states [16,23], were theoretically discovered. In contrast with infinite lattices where the polariton pairs are indeed bound states with an infinite lifetime in a qubit state, the finite lattice exhibits highly localized photon pairs with a finite lifetime that only become bound states when the periodic lattice limit is met. As experimental setups achieve a limited amount of qubits, it is relevant to explore finite systems and understand whether the highly correlated polariton pairs are the most subradiant states of the system and what the profiles of their spatial distribution are.

This class of highly correlated polariton pairs is identified by its degree of localization L based on the mode volume in optical cavities [36] and defined as

$$L = \frac{\sum_{m,n} \Psi_{m,n}^2}{(\sum_{m,n} \Psi_{m,n})^2}, \tag{10}$$

with

$$\Psi_{m,n} = \frac{1}{N^2} \sum_{i,j} (|\psi_{i,j,i+n,j+m}|^2 + |\psi_{i,j,i+n,j-m}|^2 + |\psi_{i,j,i-n,j+m}|^2 + |\psi_{i,j,i-n,j-m}|^2), \tag{11}$$

where the states $\psi_{i,j,n,m}$ and the system eigenvalues ε are obtained by direct diagonalization of Eq. (3). For the case of a state where both excitations are localized on a neighboring qubit, $L = 1$. Figure 3(a) presents this set of eigenvalues and its degree of localization of a 10×10 qubit lattice with $\varphi = 3\pi/4$, where one can notice a cluster of correlated pairs highlighted by the dashed red circle. Naturally, the presence of nonradiative decay increases the collective decay rate for the entire set of states. Its effect on the subradiant states and on the polaritons pairs can be seen in the Supplemental Material [33].

One additional way to characterize these polariton pairs is to investigate their entanglement. In particular, for bipartite systems, a powerful concept to measure the degree of entanglement between two quantum states is the von Neumann entanglement entropy, which can be defined as

$$S = \frac{-\sum_\nu |\lambda_\nu|^2 \ln |\lambda_\nu|^2}{\sum_\nu |\lambda_\nu|^2}, \tag{12}$$

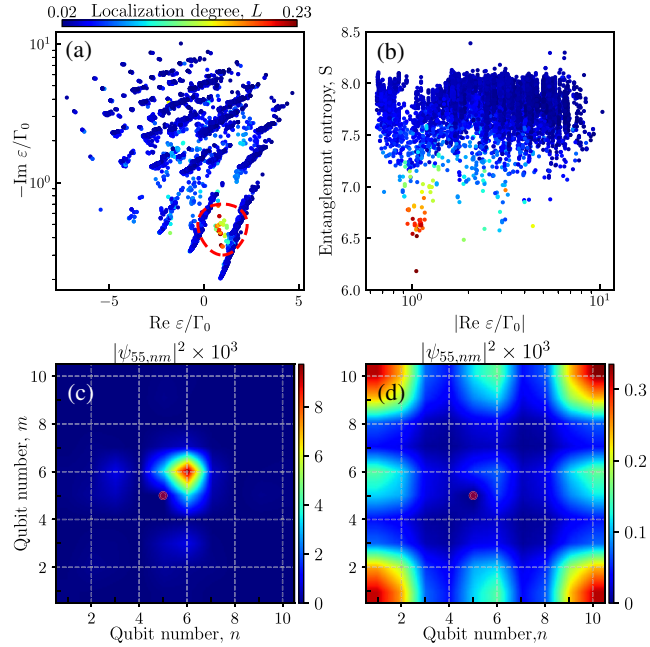

FIG. 3. (a) The two-excitation eigenvalues of the finite structure system composed of 10×10 qubits. Each eigenvalue is characterized by the localization degree L of its wave functions, in which $L \approx 1(0)$ stands for highly localized (delocalized) states. The dashed red circle highlights the highly correlated polariton states. (b) Entanglement entropy of two-polariton states: The polariton pair's spatial distribution $|\psi_{ij,nm}|^2$ of the highest localized state ($\varepsilon \approx 0.87 - 0.35i$) and the most subradiant state ($\varepsilon \approx 0.9 - 0.2i$), respectively. The polariton phase is set at $\varphi = 3\pi/4$ and the nonradiative decay is fixed at $\Gamma_{\mathrm{nr}} = 0.1\Gamma_0$. (c),(d) The probability density profile for one of the photons when the position of the second photon is fixed at the center of 10×10 qubit array (marked with red dot, (c) corresponds to the bound state and (d) to scattering state).

where λ_ν is the Schmidt coefficients obtained via the bipartite wave function rewritten using the Schmidt decomposition as $\psi_{ij,nm} = \sum_\nu \lambda_\nu \psi_{i,j} \psi_{n,m}$. It can be seen in Fig. 3(b) that the bound states correspond to the smallest entanglement entropy, reflecting the fact that these states are closest to the pure two-particle states. It can be seen in Fig. 3(c) that, for highly correlated pairs when the position of the first excitation is fixed (for example, by the measurement), the second excitation is localized in the vicinity. Conversely, the subradiant states present a delocalized pattern as shown in Fig. 3(d). Note that the two-polariton pair class is not the most subradiant state of the system. At the same time, it is known that the bound polariton pair lifetime depends crucially on the parameter φ [23]. It is therefore subject to further studies to check if there exists a "magic" value of φ for which the bound state becomes subradiant. An important implication of the obtained results is revealed if one recalls the direct mapping between the dynamics of single photons at the two-dimensional lattice and two-photon dynamics at the

one-dimensional chain. This mapping has been actively used recently to experimentally emulate quantum two-photon correlations in classical circuits [37]. This mapping can be extended to higher dimensional space: two-photon correlations at the two-dimensional lattice emulate the multiparticle correlations in 1D. Since probing of the multiparticle correlations is an extremely challenging task at the moment, the proposed structures may serve as an effective playground for the emulation of the multiparticle correlations.

To conclude, we have shown that two-photon bound polariton states exist in two-dimensional WQED systems and obtained their energy dispersion and spatial profile. These states result from the interplay between infinitely strong on-site repulsion of qubit excitations and strongly nonparabolic dispersion of the polariton modes. The bound states exist in finite two-dimensional structures of modest size and can be probed experimentally via the scattering measurements [27]. It has been recently shown that the nonparabolic dispersion of polaritons in 1D WQED structures induced by the long-range hopping leads to a plethora of peculiar physical effects ranging from interaction induced quantum Hall phases [38] to quantum chaos [21]. While up to now, the research was focused on 1D geometry, the presented emergence of the strong correlations of 2D photons indicates that 2D WQED structures may host a variety of novel yet unexplored quantum phenomena.

The main results of the paper were obtained with the support of Russian Science Foundation (Project No. 20-12-00224). The entanglement entropy has been calculated with the support of Russian Foundation of Basic research grant 20-02-00084. I. A. S. acknowledges support from Icelandic Research Fund (project "Hybrid polaritonics"). I. V. I. acknowledges the support of "Basis" Foundation (Project No. 21-1-2-61-1).

*Corresponding author.
iorsh86@yandex.ru

[1] D. Roy, C. M. Wilson, and O. Firstenberg, Colloquium: Strongly interacting photons in one-dimensional continuum, Rev. Mod. Phys. **89**, 021001 (2017).

[2] D. E. Chang, J. S. Douglas, A. González-Tudela, C.-L. Hung, and H. J. Kimble, Colloquium: Quantum matter built from nanoscopic lattices of atoms and photons, Rev. Mod. Phys. **90**, 031002 (2018).

[3] P. Trschmann, H. L. Jeannic, S. F. Simonsen, H. R. Haakh, S. Gtzinger, V. Sandoghdar, P. Lodahl, and N. Rotenberg, Coherent nonlinear optics of quantum emitters in nanophotonic waveguides, Nanophotonics **8**, 1641 (2019).

[4] A. S. Sheremet, M. I. Petrov, I. V. Iorsh, A. V. Poshakinskiy, and A. N. Poddubny, Waveguide quantum electrodynamics: collective radiance and photon-photon correlations, arXiv: 2103.06824.

[5] N. V. Corzo, J. Raskop, A. Chandra, A. S. Sheremet, B. Gouraud, and J. Laurat, Waveguide-coupled single collective excitation of atomic arrays, Nature (London) **566**, 359 (2019).

[6] A. Goban, C.-L. Hung, J. D. Hood, S.-P. Yu, J. A. Muniz, O. Painter, and H. J. Kimble, Superradiance for Atoms Trapped along a Photonic Crystal Waveguide, Phys. Rev. Lett. **115**, 063601 (2015).

[7] A. F. van Loo, A. Fedorov, K. Lalumiere, B. C. Sanders, A. Blais, and A. Wallraff, Photon-mediated interactions between distant artificial atoms, Science **342**, 1494 (2013).

[8] M. Mirhosseini, E. Kim, X. Zhang, A. Sipahigil, P. B. Dieterle, A. J. Keller, A. Asenjo-Garcia, D. E. Chang, and O. Painter, Cavity quantum electrodynamics with atom-like mirrors, Nature (London) **569**, 692 (2019).

[9] A. P. Foster, D. Hallett, I. V. Iorsh, S. J. Sheldon, M. R. Godsland, B. Royall, E. Clarke, I. A. Shelykh, A. M. Fox, M. S. Skolnick, I. E. Itskevich, and L. R. Wilson, Tunable Photon Statistics Exploiting the Fano Effect in a Waveguide, Phys. Rev. Lett. **122**, 173603 (2019).

[10] A. Sipahigil, R. E. Evans, D. D. Sukachev, M. J. Burek, J. Borregaard, M. K. Bhaskar, C. T. Nguyen, J. L. Pacheco, H. A. Atikian, C. Meuwly, R. M. Camacho, F. Jelezko, E. Bielejec, H. Park, M. Lončar, and M. D. Lukin, An integrated diamond nanophotonics platform for quantum-optical networks, Science **354**, 847 (2016).

[11] Y. Ke, A. V. Poshakinskiy, C. Lee, Y. S. Kivshar, and A. N. Poddubny, Inelastic Scattering of Photon Pairs in Qubit Arrays with Subradiant States, Phys. Rev. Lett. **123**, 253601 (2019).

[12] D. F. Kornovan, N. V. Corzo, J. Laurat, and A. S. Sheremet, Extremely subradiant states in a periodic one-dimensional atomic array, Phys. Rev. A **100**, 063832 (2019).

[13] A. Albrecht, L. Henriet, A. Asenjo-Garcia, P. B. Dieterle, O. Painter, and D. E. Chang, Subradiant states of quantum bits coupled to a one-dimensional waveguide, New J. Phys. **21**, 025003 (2019).

[14] L. Henriet, J. S. Douglas, D. E. Chang, and A. Albrecht, Critical open-system dynamics in a one-dimensional optical-lattice clock, Phys. Rev. A **99**, 023802 (2019).

[15] Y.-X. Zhang and K. Mølmer, Theory of Subradiant States of a One-Dimensional Two-Level Atom Chain, Phys. Rev. Lett. **122**, 203605 (2019).

[16] Y.-X. Zhang, C. Yu, and K. Mølmer, Subradiant bound dimer excited states of emitter chains coupled to a one dimensional waveguide, Phys. Rev. Research **2**, 013173 (2020).

[17] F. Dinc and A. M. Brańczyk, Non-Markovian super-superradiance in a linear chain of up to 100 qubits, Phys. Rev. Research **1**, 032042(R) (2019).

[18] F. Dinc, L. E. Hayward, and A. M. Brańczyk, Multidimensional super- and subradiance in waveguide quantum electrodynamics, Phys. Rev. Research **2**, 043149 (2020).

[19] E. Kim, X. Zhang, V. S. Ferreira, J. Banker, J. K. Iverson, A. Sipahigil, M. Bello, A. Gonzalez-Tudela, M. Mirhosseini, and O. Painter, Quantum Electrodynamics in a Topological Waveguide, Quantum Electrodynamics in a Topological Waveguide, Phys. Rev. X **11**, 011015 (2021).

[20] J. Perczel, J. Borregaard, D. E. Chang, S. F. Yelin, and M. D. Lukin, Topological Quantum Optics Using Atomlike

Emitter Arrays Coupled to Photonic Crystals, Phys. Rev. Lett. **124**, 083603 (2020).

[21] A. V. Poshakinskiy, J. Zhong, and A. N. Poddubny, Quantum Chaos Driven by Long-Range Waveguide-Mediated Interactions, Phys. Rev. Lett. **126**, 203602 (2021).

[22] K. M. Birnbaum, A. Boca, R. Miller, A. D. Boozer, T. E. Northup, and H. J. Kimble, Photon blockade in an optical cavity with one trapped atom, Nature (London) **436**, 87 (2005).

[23] A. N. Poddubny, Quasiflat band enabling subradiant two-photon bound states, Phys. Rev. A **101**, 043845 (2020).

[24] S. Mahmoodian, G. Calajó, D. E. Chang, K. Hammerer, and A. S. Sørensen, Dynamics of Many-Body Photon Bound States in Chiral Waveguide QED, Phys. Rev. X **10**, 031011 (2020).

[25] J. Zhong, N. A. Olekhno, Y. Ke, A. V. Poshakinskiy, C. Lee, Y. S. Kivshar, and A. N. Poddubny, Photon-Mediated Localization in Two-Level Qubit Arrays, Phys. Rev. Lett. **124**, 093604 (2020).

[26] J. Zhong and A. N. Poddubny, Classification of three-photon states in waveguide quantum electrodynamics, Phys. Rev. A **103**, 023720 (2021).

[27] M. Gong, S. Wang, C. Zha, M.-C. Chen, H.-L. Huang, Y. Wu, Q. Zhu, Y. Zhao, S. Li, S. Guo *et al.*, Quantum walks on a programmable two-dimensional 62-qubit superconducting processor, Science **372**, 948 (2021).

[28] A. González-Tudela and J. I. Cirac, Quantum Emitters in Two-Dimensional Structured Reservoirs in the Nonperturbative Regime, Phys. Rev. Lett. **119**, 143602 (2017).

[29] A. González-Tudela, C.-L. Hung, D. E. Chang, J. I. Cirac, and H. Kimble, Subwavelength vacuum lattices and atom–atom interactions in two-dimensional photonic crystals, Nat. Photonics **9**, 320 (2015).

[30] O. Astafiev, A. M. Zagoskin, A. Abdumalikov, Y. A. Pashkin, T. Yamamoto, K. Inomata, Y. Nakamura, and J. S. Tsai, Resonance fluorescence of a single artificial atom, Science **327**, 840 (2010).

[31] Z. K. Minev, K. Serniak, I. M. Pop, Z. Leghtas, K. Sliwa, M. Hatridge, L. Frunzio, R. J. Schoelkopf, and M. H. Devoret, Planar Multilayer Circuit Quantum Electrodynamics, Phys. Rev. Applied **5**, 044021 (2016).

[32] D. E. Chang, V. Gritsev, G. Morigi, V. Vuletić, M. D. Lukin, and E. A. Demler, Crystallization of strongly interacting photons in a nonlinear optical fibre, Nat. Phys. **4**, 884 (2008).

[33] See Supplemental Material at http://link.aps.org/supplemental/10.1103/PhysRevLett.127.273602 for the derivation of the two-particle Schrödinger equation (S1), (S2) dispersion relation calculation, (S3) Real-space profile of the bound state, (S4) and the effect of non-radiative decay on the two-polariton localization.

[34] K. Winkler, G. Thalhammer, F. Lang, R. Grimm, J. Hecker Denschlag, A. J. Daley, A. Kantian, H. P. Büchler, and P. Zoller, Repulsively bound atom pairs in an optical lattice, Nature (London) **441**, 853 (2006).

[35] E. Economou, *Greens Functions in Quantum Physics*, Springer Series in Solid-State Sciences (Springer, Berlin, Heidelberg, 2013).

[36] P. T. Kristensen and S. Hughes, Modes and mode volumes of leaky optical cavities and plasmonic nanoresonators, ACS Photonics **1**, 2 (2014).

[37] N. A. Olekhno, E. I. Kretov, A. A. Stepanenko, P. A. Ivanova, V. V. Yaroshenko, E. M. Puhtina, D. S. Filonov, B. Cappello, L. Matekovits, and M. A. Gorlach, Topological edge states of interacting photon pairs emulated in a topolectrical circuit, Nat. Commun. **11**, 1436 (2020).

[38] A. V. Poshakinskiy, J. Zhong, Y. Ke, N. A. Olekhno, C. Lee, Y. S. Kivshar, and A. N. Poddubny, Quantum Hall phases emerging from atom–photon interactions, npj Quantum Inf. **7**, 34 (2021).